

# CFD of Transition from Bubbly Flow to Slug Flow in Vertical Pipe

Zhi Shang, Jing Lou, Hongying Li

Institute of High Performance Computing (IHPC), Agency for Science, Technology and Research, Singapore

## Abstract

The transitional regimes of two-phase flow are widely met in many industrial practices. The phenomena of the transition flows are very complex. How to measure and simulate the transition flows are really challenging to the engineers. In this paper, the new Lagrangian algebraic slip mixture model (LASMM) was employed to quantify the transitional regimes of two-phase flow in a vertical pipe. In the application of this model, the typical flow transition from bubbly flow to slug flow was simulated. Through the comparisons to the experiment data, it confirms the validity and applicability of LASMM on the simulation of the transitional regime of two-phase flow.

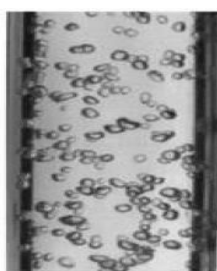
**Keyword:** LASMM, transition flow, two-phase flow, vertical pipe

**Corresponding author:** E mail ID: shangz@ihpc.a-star.edu.sg

## INTRODUCTION

Multiphase flows appear in various industrial processes and in the petroleum industry. Particularly, in where oil, gas and water are often produced and transported together<sup>[1]</sup>. During co-current flow in a pipe the multiphase flow topology can

acquire a variety of characteristic distributions called flow regimes, or flow patterns, each featuring specific hydrodynamic characteristics (e.g. bubbly, slug, churn, annular, shown in Figure 1), depending on the volumetric flow rates of the gas.



(a) Bubbly Flow



(b) Slug Flow



(c) Churn Flow



(d) Annular Flow

**Fig. 1:** Flow Patterns of Gas-Water Two-Phase Flow.

Some of these hydrodynamic features are clearly undesirable particularly in the hydrocarbon transportation systems, for example slug flow, which may be harmful to some operations components. Such multiphase flows exist in oil and gas pipes. In gas & oil industry, the flow patterns

to and from the reservoir, too. Indeed, in extraction and injection processes of oil and gas to and from reservoirs, multiphase mixtures of oil, natural gas and water is piped between the reservoir and the surface.

were used to help the oil extraction, for

example gas-lift technique, shown in Figure 2<sup>[2]</sup>. In the gas-lift technique, gas is injected at the bottom of a production pipe (through which oil and water are flowing) in order to reduce the gravitational pressure drop in the well. This results in an increase of the oil flow rate in the pipe. In practice, gas is injected from valves attached to the pipe wall, which generates large bubbles. The gravitational pressure drop is then reduced because

1. The rise velocity of small bubbles is lower, and hence the residence time and void fraction in the pipe are higher.
2. Small bubbles are more evenly distributed over the cross-section of the pipe, which increases the gas void fraction.
3. Small bubbles postpone the transition from bubbly flow to slug flow, which is an undesirable operating condition for gas-lift.

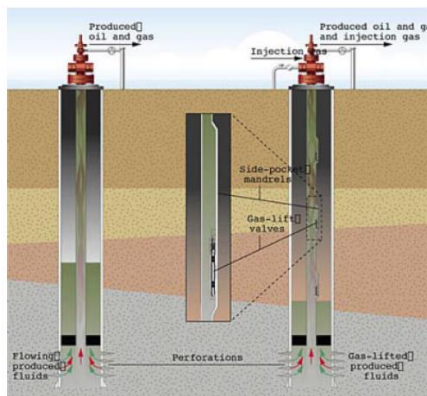


**Fig. 2:** Cross-Section of Wells Employing Gas lift (Schlumberger)<sup>[2]</sup>.

A good knowledge of the fluid mechanics in general and flow distribution there should have a significant impact on the well productivity, well storage capacity, production costs and equipment size. Typically the transitional flow will affect the flow behaviors. In practical industry, the transitional flow will be the option basis of the operating flow regimes<sup>[3]</sup>. Therefore the studies of the transitional flows have a great significance on practical multiphase flow.

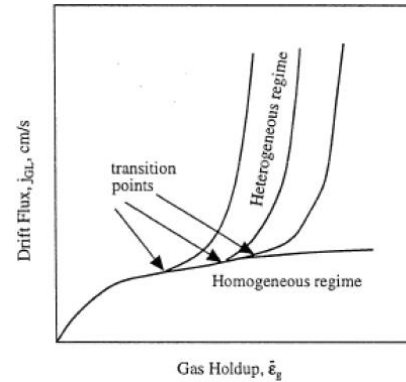


**Fig. 3:** Transition Gas Holdup vs. Drift Flux Plot.

The transitional flow will be affected by the gas void fraction. Figure 3 shows the experiment done by Wallis<sup>[4]</sup>. From Figure 3, it can be seen that the three main transitions occur between at certain gas void fractions. Later, Szalinski *et al.*<sup>[5]</sup> and Mo *et al.*<sup>[6]</sup> did the experiments for the transitional two-phase flows in a vertical pipe, shown in Figure 4. From Figure 4 it can be seen that following the increase of the void fraction, the transitions from bubbly flow to slug flow ( $\alpha_g = 0.3$ ), from slug flow to churn flow ( $\alpha_g = 0.6$ ) and from churn flow to annular flow ( $\alpha_g = 0.8$ ) will happen at certain regions of the void fraction.

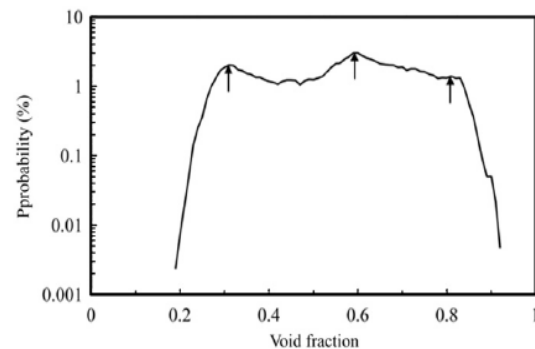


**Fig. 4:** Experiment of Flow Transition Regimes at Peak Point of the Probability Density.

Further, new possibilities and challenges for advanced computational multiphase flow are offered today in flow assurance where various complex issues in particular as to the transport appear and need to be addressed. In this paper, the heterogeneous mixture model, Lagrangian algebraic slip

mixture model (LASMM)<sup>[7]</sup>, was employed to quantity study the phenomena of the transitional flows, which include the transitions from bubbly flow to slug flow, from slug flow to churn flow and from churn flow to annular flow, based on the advanced computational technology of CFD.

## MATHEMATICAL MODELING

Considering a problem of turbulent multi-component multi-phase flow with one continuous phase and several dispersed phases, the time average conservation equations of mass, momentum and energy for the LASMM as well as the turbulent kinetic energy equation and the turbulent kinetic energy transport equation can be written as the following<sup>[7]</sup>.

$$\partial \rho_m / \partial t + \nabla \cdot (\rho_m \mathbf{U}_m) = 0 \quad \text{Eq. (1)}$$

$$\partial (\rho_m \mathbf{U}_m) / \partial t + \nabla \cdot (\rho_m \mathbf{U}_m \mathbf{U}_m) = -\nabla p + \rho_m \mathbf{g} + \nabla \cdot \left[ \left( \mu_m + \mu_t \right) (\nabla \mathbf{U}_m + \nabla \mathbf{U}_m^T) \right] - \nabla \cdot \sum \alpha_k \rho_k \mathbf{U}_{km} \mathbf{U}_{km} \quad \text{Eq. (2)}$$

$$\partial (\rho_m e_m) / \partial t + \nabla \cdot (\rho_m \mathbf{U}_m h_m) = q + \nabla \cdot \left[ \left( \frac{\mu_m}{Pr} + \frac{\mu_t}{Pr_t} \right) \nabla h_m \right] - \nabla \cdot \sum \alpha_k \rho_k h_k \mathbf{U}_{km} \quad \text{Eq. (3)}$$

$$\partial (\rho_m k) / \partial t + \nabla \cdot (\rho_m \mathbf{U}_m k) = \nabla \cdot \left[ \left( \mu_m + \frac{\mu_t}{\sigma_k} \right) \nabla k \right] + G - \rho_m \varepsilon \quad \text{Eq. (4)}$$

$$\partial (\rho_m \varepsilon) / \partial t + \nabla \cdot (\rho_m \mathbf{U}_m \varepsilon) = \nabla \cdot \left[ \left( \mu_m + \frac{\mu_t}{\sigma_\varepsilon} \right) \nabla \varepsilon \right] + \frac{\varepsilon}{k} (C_1 G - C_2 \rho_m \varepsilon) \quad \text{Eq. (5)}$$

Where

$$\rho_m = \sum \alpha_k \rho_k \quad \text{Eq. (6)}$$

$$\mu_m = \sum \alpha_k \mu_k \quad \text{Eq. (7)}$$

$$\rho_m \mathbf{U}_m = \sum \alpha_k \rho_k \mathbf{U}_k \quad \text{Eq. (8)}$$

$$\mathbf{U}_{km} = \mathbf{U}_k - \mathbf{U}_m \quad \text{Eq. (9)}$$

$$G = \frac{1}{2} \mu_t (\nabla \mathbf{U}_m + \nabla \mathbf{U}_m^T) : \nabla \mathbf{U}_m \quad \text{Eq. (10)}$$

$$\mu_t = C_\mu \rho_m \frac{k^2}{\varepsilon} \quad \text{Eq. (11)}$$

where,  $\rho$  is the density,  $\mathbf{U}$  are the velocity vectors,  $\alpha$  is the volumetric fraction,  $p$  is pressure,  $\mathbf{g}$  is the gravitational acceleration vector,  $\mathbf{U}_{km}$  is the diffusion velocity vector of  $k$  dispersed phase relative to the averaged mixture flow,  $e$  is internal energy,  $h$  is enthalpy,  $q$  is heat input,  $\mu$  is viscosity,  $\mu_t$  is turbulent viscosity,  $Pr$  is molecular Prandtl number,  $Pr_t$  is turbulent Prandtl number,  $G$  is stress production.  $C_\mu$ ,

$\sigma_k$ ,  $\sigma_\varepsilon$ ,  $C_1$ ,  $C_2$  are constants for standard  $k$ - $\varepsilon$  turbulence model<sup>[8]</sup>, shown in Table 1. The subscript  $m$  stands for the averaged mixture flow, and  $k$  stands for  $k$  dispersed phase.

**Table 1:** Constants of Standard  $k$ - $\varepsilon$  Turbulence Model.

variable	$C_\mu$	$\sigma_k$	$\sigma_\varepsilon$	$C_1$	$C_2$
constant	0.09	1.0	1.3	1.44	1.92

Additional to the above equations, the

following conservation equation for each phase is also necessary.

$$\partial(\alpha_k \rho_k) / \partial t + \nabla \cdot (\alpha_k \rho_k \mathbf{U}_m) = \Gamma_k - \nabla \cdot (\alpha_k \rho_k \mathbf{U}_{km}) \quad \text{Eq. (12)}$$

Where  $\Gamma_k$  is the generation rate of k-phase. In order to closure the governing Eq.s (1-12), it is necessary to determine the diffusion velocities  $\mathbf{U}_{km}$ . The following equation is employed to covert the diffusion velocities to slip velocities that can be defined as  $\mathbf{U}_{kl} = \mathbf{U}_k - \mathbf{U}_l$ .

$$\mathbf{U}_{km} = \mathbf{U}_{kl} - \sum \frac{\alpha_k \rho_k}{\rho_m} \mathbf{U}_{kl} \quad \text{Eq. (13)}$$

Actually the above equation can be developed from the definition of the mixture density Eq. (6), the definition of

$$\mathbf{F}_g = \mathbf{F}_{\text{buoyancy}} + \mathbf{F}_{\text{drag}} + \mathbf{F}_{\text{virtual}} + \mathbf{F}_{\text{lif}} + \mathbf{F}_{\text{lubrication}} + \mathbf{F}_{\text{dispersion}} + \dots \quad \text{Eq. (14)}$$

where  $\mathbf{F}_g$  is the inertia force acting on the bubble due to its acceleration,  $\mathbf{F}_{\text{buoyancy}}$  is the force due to gravity and buoyancy,  $\mathbf{F}_{\text{drag}}$  is force due to drag by the continuous liquid,  $\mathbf{F}_{\text{virtual}}$  is the force due to virtual mass effect,  $\mathbf{F}_{\text{lif}}$  is the force due to transverse lift,  $\mathbf{F}_{\text{lubrication}}$  is the wall lubrication force caused by the liquid flow rate which between gas bubble and the solid wall is lower than between the gas bubble and the main flow,  $\mathbf{F}_{\text{dispersion}}$  is the

mixture mass flux Eq. (8), the diffusion velocity Eq. (9) and the slip velocity  $\mathbf{U}_{kl}$ . Once the slip velocities are obtained, the whole governing equations will be closed.

Because the slip velocities present the difference of the movement between the dispersed phase for instance gas and the continuous phase for instance liquid. The dispersed phase can be presented by its own law of motion. For example, in gas and liquid two-phase flow system, the following equation can be use to describe the single bubble movement inside a liquid, which normally is called as Lagrangian equation of motion.

turbulent dispersion force due to the movement of the turbulent eddies, and so on the other forces can be added into Eq. (14).

In this paper, only the forces of buoyancy, drag, virtual mass, transverse lift, wall lubrication and turbulent dispersion were considered. The expanded description about these forces can be represented as in the following equations<sup>[9-11]</sup>.

$$\mathbf{F}_g = \rho_g \frac{d\mathbf{U}_g}{dt} \quad \text{Eq. (15)}$$

$$\mathbf{F}_{\text{buoyancy}} = (\rho_g - \rho_l) \mathbf{g} \quad \text{Eq. (16)}$$

$$\mathbf{F}_{\text{drag}} = \frac{3\rho_l C_d}{4d_g} (\mathbf{U}_l - \mathbf{U}_g) |\mathbf{U}_l - \mathbf{U}_g| \quad \text{Eq. (17)}$$

$$\mathbf{F}_{\text{lif}} = C_l \rho_l (\mathbf{U}_l - \mathbf{U}_g) \times \nabla \times \mathbf{U}_l \quad \text{Eq. (18)}$$

$$\mathbf{F}_{\text{virtual}} = C_{vm} \rho_l \left( \frac{d\mathbf{U}_l}{dt} - \frac{d\mathbf{U}_g}{dt} \right) \quad \text{Eq. (19)}$$

$$\mathbf{F}_{\text{lubrication}} = C_w \rho_l \left[ (\mathbf{U}_l - \mathbf{U}_g) - ((\mathbf{U}_l - \mathbf{U}_g) \cdot \mathbf{n}_w) \mathbf{n}_w \right]^2 \max \left( 0, \frac{C_{w1}}{d_g} + \frac{C_{w2}}{y_w} \right) \mathbf{n}_w \quad \text{Eq. (20)}$$

$$\mathbf{F}_{\text{dispersion}} = C_{td} \rho_l k \frac{\nabla \alpha_l}{\alpha_g} \quad \text{Eq. (21)}$$

where, in Eq.s (15–21),  $g$  is gravity,  $d_g$  is bubble diameter,  $y_w$  is the distance to the nearest wall,  $n_w$  is the unit normal pointing away from the wall.  $C_d$  is drag force coefficient,  $C_{vm}$  is virtual force coefficient,  $C_l$  is lift force coefficient,  $C_w$  is the wall lubrication force coefficient,  $C_{w1}$  and  $C_{w2}$  are the wall lubrication constants, and  $C_{td}$  is the turbulent dispersion coefficient.

$$U_{gl} = -\frac{4(\rho_1 - \rho_g)d_g}{3\rho_1 C_d |U_1 - U_g|} \left[ g - \frac{(F_{\text{virtual}} + F_{\text{lift}} + F_{\text{lubrication}} + F_{\text{dispersion}})}{(\rho_1 - \rho_g)} + \frac{\rho_g}{(\rho_1 - \rho_g)} \frac{dU_g}{dt} \right] \quad \text{Eq. (22)}$$

Further if we define the Reynolds number of the gas bubble as in Eq. (23) and the relax time of the dispersed phase to reach

$$\text{Re}_b = \frac{\rho_m |U_1 - U_g| d_g}{\mu_m} \quad \text{Eq. (23)}$$

$$\tau_g = \frac{\rho_g \rho_m d_g^2}{18 \rho_l \mu_m} \quad \text{Eq. (24)}$$

$$U_{gl} = -\frac{\tau_g (\rho_1 - \rho_g)}{f_{\text{drag}} \rho_g} \left[ g - \frac{(F_{\text{virtual}} + F_{\text{lift}} + F_{\text{lubrication}} + F_{\text{dispersion}})}{(\rho_1 - \rho_g)} + \frac{\rho_g}{(\rho_1 - \rho_g)} \frac{dU_g}{dt} \right] \quad \text{Eq. (25)}$$

In Eq. (25),  $f_{\text{drag}}$  is the drag function that can be defined as:

$$f_{\text{drag}} = \frac{C_d \text{Re}_b}{24} \quad \text{Eq. (26)}$$

## INTERFACIAL FORCE COEFFICIENTS

Owing to the novel LASMM considering the interfacial forces between dispersed and continuous phases, the slip velocity was able to deal with the non-uniform movement of bubbles. However the interfacial forces, such as drag force, lift force, virtual mass force, wall lubrication force, and turbulent dispersion force and so on, have to be modeled before the simulations. The specific formulas about these forces are presented in Eq.s (15-21). From the Equation, it can be seen that once the coefficients of the forces are determined, the numerical simulation will be able to be performed. Normally all the

These coefficients can be determined by empirical formulas or constants.

If we define the dispersed phase as gas, the slip velocity of  $U_{kl}$  in Eq. (13) will be the slip velocity between gas and liquid as  $U_{gl}$ . The specific slip velocity between gas and liquid can be developed from Eq. (14) as the following.

the terminal velocity as in Eq. (24), the final slip velocity should become the form as in Eq. (25).

coefficients, such as drag force coefficient, virtual mass force coefficient, lift force coefficient, wall lubrication force coefficient and turbulent dispersion force coefficient, can be formulized as the functions of some non-dimensional numbers, for example Reynolds number and Eötvös number. All the coefficients used in this paper are same as Shang *et al.*<sup>[7]</sup>.

## MODELING BUBBLE SIZE DISTRIBUTION

Since the slip velocity is determined, the whole equations are closed to be solved. Considering the bubble size could be changed due to breakup and coalescence,

same as<sup>[12, 13]</sup>, the following experimental formula can be employed to estimate the distributions of the bubble size<sup>[14]</sup>.

$$d_g = 3g^{-0.44} \sigma^{0.34} \mu_l^{0.22} \rho_l^{-0.45} \rho_g^{-0.11} u_g^{-0.02} \quad \text{Eq. (27)}$$

Where  $d_g$  is bubble size,  $g$  is gravity,  $\sigma$  is surface tension,  $\mu_l$  is liquid viscosity,  $\rho_l$  is liquid density,  $\rho_g$  is gas density and  $u_g$  is superficial gas velocity.

## NUMERICAL SIMULATIONS

During the numerical simulations, the CFD technique was based on ANSYS FLUENT 15.0. The drag force model was

accomplished using the concept of user defined functions (UDF). All the simulations are performed under transient running until steady state and the time step was set up from  $1.0 \times 10^{-6}$  to  $1.0 \times 10^{-3}$  seconds according to the Courant number requirement.

Krepper *et al.*<sup>[15]</sup> used an electrode wire-mesh sensor to study the transitional flow from bubbly flow to slug flow. The transition occurred at the gas volume fraction around 0.3. Figure 5 shows the state of the transitional flow between bubbly flow and slug flow.

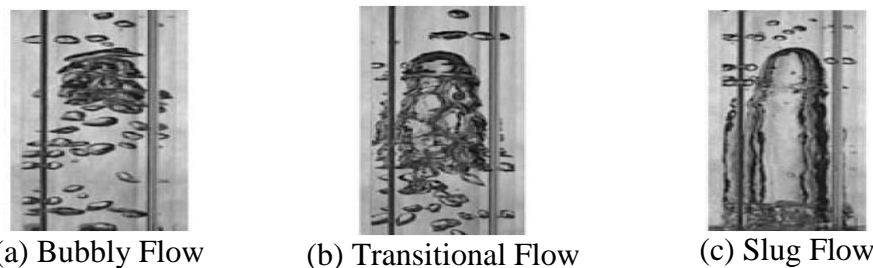


**Fig. 5: Transition between Bubbly Flow and Slug Flow.**

For keeping the coincident of comparisons, in Krepper *et al.*<sup>[15]</sup> upward flows,  $r/R = 0.0$  is the pipe's center and  $r/R = 1.0$  is the pipe's wall. Fig. 6 shows the profile comparisons of the gas volume fraction ( $\alpha_g$ ) simulated by the current model to the experiments<sup>[15]</sup> at the cross section of  $L/D = 60$  for upward flows. The flow conditions are the regimes of  $j_g = 0.342$  m/s and  $j_l = 1.0$  m/s.

From Figure 6, it can be seen that the gas volume fraction ( $\alpha_g$ ) was core peak distributed. The simulations have consistent predictions in both of the flow regimes compared to the experiments. In Figure 6, the peak value of the gas volume fraction reaches above 0.4. From the maximum value of the gas volume fraction, it can be deduced that the flow regime may cover the transition region from bubbly flow to slug flow. Unfortunately, Krepper *et al.*<sup>[15]</sup> only measured the data of gas volume fractions.

It therefore can only compare the distributions of gas volume fractions for the validations.

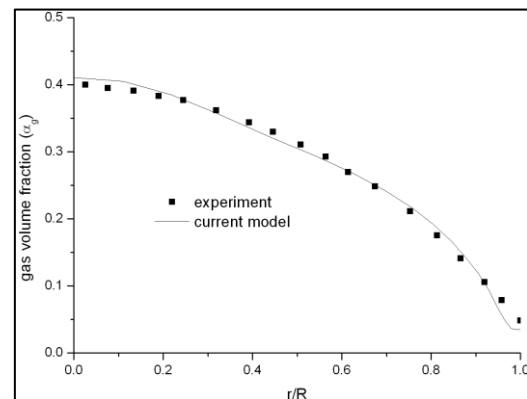


**Fig. 6: Comparisons of the Gas Volume Fraction Between Experiment and Simulation.**

## CONCLUSION

From the simulations of the heterogeneous mixture model (LASMM) can be used to study the transitional phenomena of gas-water two-phase flow. Through the comparisons between the experiment and

simulations, it is confirmed that the heterogeneous mixture model developed in this paper is able to simulate the complex multiphase flows in oil & gas industry including the transition flows. It lays the fundemants for the future practical industrial application.

### ACKNOWLEDGMENTS

The authors would like to thank the support by Multiphase Flow for Deep-Sea Oil & Gas Down-hole Applications–SERC TSRP Programme of Agency for Science, Technology and Research (A\*STAR) in Singapore (Ref # 102 164 0075).

### REFERENCES

- Hewitt G.F. Three-phase gas-liquid-liquid flows in the steady and transient states. *Nuclear Engineering Design*. 2005; 235: 1303–16p.
- Lakehal D. Advanced simulation of transient multiphase flow & flow assurance in the oil & gas industry. *The Canadian Journal of Chemical Engineering*. 2013; 9999, 1–14p.
- Guet S., Ooms G., Oliemans R.V.A., *et al.* Bubble injector effect on the gas lift efficiency, *AIChE Journal*. 2003; 49(9): 2242–52p.
- Wallis G.B. One-dimensional Two-phase Flow. *McGraw-Hill*. New York USA, 1969.
- Szalinski L., Abdulkareem L.A., Silva M.J.D., *et al.* Comparative study of gas-oil and gas-water two-phase flow in a vertical pipe. *Chemical Engineering Science*. 2010; 65: 3836–48p.
- Mo S., Ashrafiyan A., Johansen S.T. Simulation of flow regime transitions in vertical pipe flow. *8th International Conference on Multiphase Flow*; 2013 May 26–31; Jeju, Korea.
- Shang Z., Lou J., Li H. A novel Lagrangian algebraic slip mixture model for two-phase flow in horizontal pipe. *Chemical Engineering Science*. 2013; 102: 315–23p.
- Launder B.E., Spalding D.B. The numerical computation of turbulent flows. *Comp. Meth. Appl. Meth. Eng.* 1974; 3: 269–89p.
- Lain S., Broder D., Sommerfeld M., *et al.* Modelling hydrodynamics and turbulence in a bubble column using the Euler-Lagrange procedure. *Int. J. Multiphase Flow*. 2002; 28: 1381–1407p.
- Zhou L.X., Yang M., Lian C.Y., *et al.* On the second-order moment turbulence model for simulating a bubble column. *Chemical Engineering Science*. 2002; 57: 3269–81p.
- Yeoh G.J., Tu J.Y., Numerical modeling of bubbly flows with and without heat and mass transfer. *Applied Mathematical Modelling*. 2006; 30: 1067–95p.
- Chen P. *Modeling the fluid dynamics of bubble column flows*, Ph. D thesis, Washington University, USA, 2004.
- Chen P., Dudukovic M.P., Sanyal J. Three-dimensional simulation of bubble column flows with bubble coalescence and breakup. *AIChE J.* 2005; 51(3): 696–712p.
- Wilkinson P.M. *Physical aspects and scale-up of high pressure bubble columns*. Netherlands: University of Groningen; 1991.
- Krepper E., Lucas D., Prasser H.M. On the modeling of bubbly flow in vertical pipes. *Nuclear Engineering and Design*. 2005; 235: 597–611p.